Spectral Sensitization of TiO_2 Nanocrystalline Electrodes with Aggregated Cyanine Dyes

A. Ehret, L. Stuhl, and M. T. Spitler*

ChemMotif, Inc., 60 Thoreau Street, #211, Concord, Massachusetts 01742

Received: May 22, 2001; In Final Form: August 7, 2001

New chromophores were explored for use in dye-sensitized solar cells. The attachment of various di-carboxylated cyanine dyes to nanocrystalline TiO_2 was examined spectroscopically and through their performance in a sensitized solar cell. It was found that aggregated forms of these cyanine dyes sensitized with an efficiency equal to that of the monomer form and that combinations of cyanine dyes could be used to sensitize solar cells over the entire visible spectrum. With the high extinction coefficients of the organic dyes, short circuit photocurrents for these cyanine-sensitized systems was maximized at a 4 μm thickness of the nanocrystalline TiO_2. Short circuit photocurrents for these 4 μm solar cells were found to exceed that of ruthenium coordination complexes.

Recent advances in the development of dye-sensitized solar cells have focused on the nanocrystalline TiO_2 cells sensitized by Ru(II) coordination complexes. Grätzel first combined these sensitizers and the TiO_2 substrate to make such a solar cell and has improved its performance to the point where a 10% power conversion has been achieved.[1] It offers many advantages as a solar cell. The materials are low in cost and it is easy to assemble, requiring only simple coating and sintering procedures.[2]

Many sensitizers have been used in this application, but few have matched the performance of the dithiacyanato-bis(dicarboxy-bipyridyl)Ru(II) (**N3**) compound on the nanocrystalline TiO_2.[1] Grätzel has reported the use of another Ru(II) complex, [2,2′-6′2″-terpyrididine-4,4′,4″-tricarboxylic Ru(II)$(NCS)_3]^-$,[3] that has spectral features that extend over a broader range of the visible spectrum than the **N3** dye. In a solar cell, it produces conversion efficiencies comparable to the **N3** species.

In many ways, this solar cell has been optimized for use of these particular ruthenium sensitizers. Specific concentrations of reducing agents, solvents, and particular preparations of TiO_2 colloids have been found for use with the **N3** chromophore that maximize power conversion. While very pragmatic, such optimization procedures have not provided a complete picture of the mechanistic aspects of the sensitization process. In this situation, a screening process to uncover new sensitizers that involves a simple substitution of candidate chromophores for the ruthenium complexes may not be effective. In principle, the parameters of the solar cell must be optimized for each dye; in practice, this consumes too much time. The result is the limited selection of suitable alternatives for study in dye-sensitized solar cells.

Even with the present optimization of these solar cells, the **N3**-sensitized cell is limited by the spectral characteristics of a coordination complex with a low oscillator strength. A 10 μm thick TiO_2 layer is required in the cells in order for the extinction of the cell to be large enough to absorb a significant fraction of the incident light. Although the **N3** complex has a broad absorption spectrum, it absorbs weakly in the red. 2,2′-6′2″-Terpyrididine-4,4′,4″-tricarboxylic Ru(II)$(NCS)_3$- was developed to rectify this situation through an extended absorption in the red, but its extinction coefficient is still low, and a 10 μm thick cell is required to make a truly black cell.[3]

It is well-known that organic dyes have much higher oscillator strengths than these metal coordination complexes. Their use would allow a correspondingly thinner layer of TiO_2 to effect an equivalent light harvesting. However, the organic dyes have shown very little promise in this application.[4−14] Single organic dyes can have oscillator strengths that approach unity. However, they absorb only a 50 nm wide region of the visible spectrum. Their light harvesting is very poor. This absorption can be broadened thorugh aggregation, which has been explored with both the blue-shifted H-aggregates and red-shifted J-aggregates of merocyanine dyes,[15,16] but AM1 solar conversion efficiencies have failed to reach 1%.

This work will show that organic chromophores can be used in these dye-sensitized solar cells to produce short circuit photocurrents and conversion efficiencies comparable to that of control **N3** cells. Thiacyanine and oxacyanine dyes are introduced that have two carboxyl functions for chelation to the nanocrystalline TiO_2. The higher oscillator strength of these dyes will allow for a thinner solar cell and open the possibility of substitution of regenerating systems other than the acetonitrile iodide/iodine system.

It is clear that, however, that the narrow spectral width of each of these dyes will require the use of a mixture of several such dyes to cover the visible spectrum. We show that such a spectral sensitization package of several dyes can be assembled and attached to nanocrystalline TiO_2.

The implications of this work are clear: there are many possible organic sensitizers for dye-sensitized solar cells and the range of their redox characteristics, both in the ground and excited state, will allow for optimization of the solar cell with materials different from those presently in use.

Experimental Section

The structures of the dyes used in this work are given in Figure 1. The dyes were synthesized through procedures that have been described in previous work.[17]

Redox potentials of these dyes were determined using second harmonic AC voltammetry using a Pt working electrode with a 1.6 mm radius.[18] The measurements were done in acetonitrile

* Corresponding author. E-mail: spitlem@tiac.net.

10.1021/jp011952+ CCC: $20.00 © 2001 American Chemical Society
Published on Web 09/20/2001

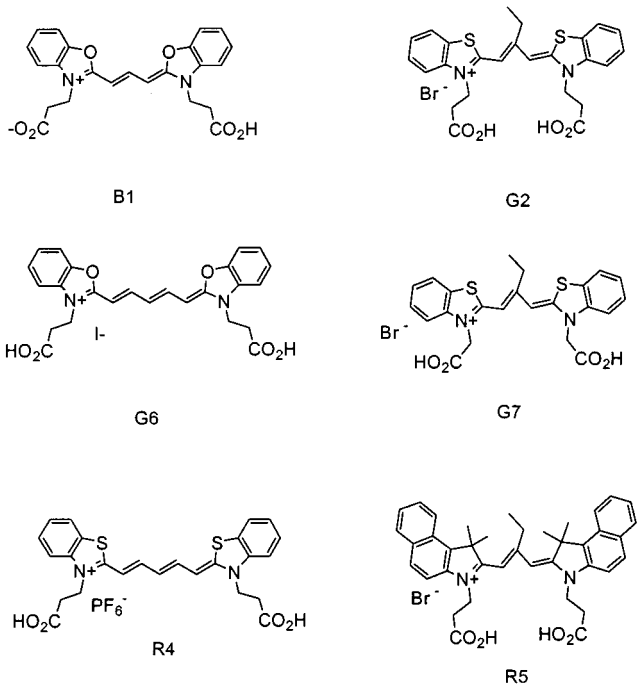

Figure 1. Structures of the cyanine dyes used in this work.

with 0.10 M tetrabutylammonium tetrafluoroborate using a Ag^+/Ag reference electrode that was calibrated against ferrocene. The bromide salts were exchanged with BF_4^- through dissolution of the dye with aqueous KOH and precipitation with aqueous HCl in the presence of excess $NaBF_4$. Potentials for particular dyes were measured with reference to the dye 2,2′-diethyldithiacarbocyanine, which is known to have an oxidation potential of +0.902 V vs Ag/AgCl.[18] Reproducibility of the potentials was ±5 mV.

The TiO_2 preparation was made using titanium isopropoxide and nitric acid after the manner of Gratzel.[19] The initial colloid preparation was ripened through heating the solution in a sealed pressure vessel at 200 °C with stirring for sixteen hours. The solution was concentrated and a carbowax 20M binder was added to 40 wt % of the TiO_2. As a surfactant, BASF Pluronic P103, an ethylene oxide/propylene oxide triblock copolymer, was used at a 0.5% level. The final solution was 15 wt % of TiO_2; it was not sonicated prior to coating.

The TiO_2 preparation was spread on one inch square conductive SnO_2 glass using wire wound Mayer rods to control the coating thickness. The rods used in this work resulted in coatings with a nominal thickness of 6, 15, 27, 35, 54, and 69 μm. Following coating, the samples were allowed to dry and then heated to 450 °C in 30 min and held there for a further 30 min. The final TiO_2 layer thicknesses were measured with a Dektak Profilometer to be 0.9, 2.3, 3.9, 5.1, 8.1, and 10.5 μm (± 5%).

Solar cells were made with these dyed nanocrystalline layers by mating them with another 8 ohm inch square SnO_2 element and sealing with low temperature, hot melt glue, leaving apertures for insertion of electrolyte. The counter electrode was platinized through a coating of a thin layer of chloroplatinic acid solution and subsequent heating at 200 °C for 10 min. The standard electrolyte composition of 0.50 M NaI/0.05 M I_2 in acetonitrile was used.[1] The electrolyte was added to the cell prior to exposure and allowed to sit for several minutes before exposure and measurement.

A 250 W tungsten light source provided the light for exposure. The beam was passed through a water filter and a 420 nm cutoff filter and provided an incident power of 110 mW/cm^2. Relative to a xenon lamp, the spectral distribution of this photon flux is low in the blue end of the spectrum and slightly higher in the red end. The current−voltage curves were measured using an electronic instrument built in house.

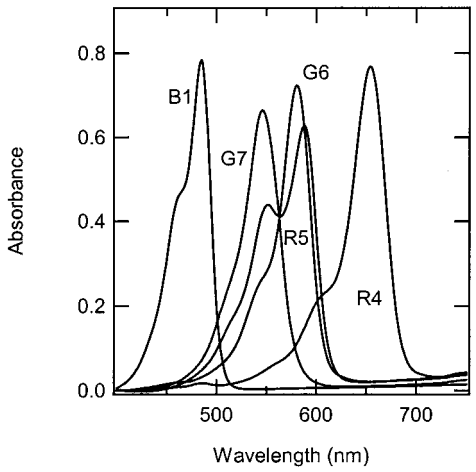

Figure 2. Solution spectra of the dyes of Figure 1 show that their absorption spans the visible from 400 to 700 nm. The spectra were recorded in methanol at concentrations that ranged from 5×10^{-6} M to 1×10^{-5} M. The spectrum of G2 overlays that of G7 and is not given here.

Results

The intent of this work is to assess the relative performance of the **N3** chromophore and cyanine dyes as spectral sensitizers for nanocrystalline TiO_2 solar cell. Aside from a higher oscillator strength, the organic chromophores have a range of absorption energies and redox potentials that would allow optimization of the nanocrystalline solar cell with different materials than are presently compatible with the **N3**/TiO_2 system.

The absorption spectra of the dyes used in this work are given in Figure 2 for the dyes in methanol and are seen to span the visible spectrum. The absorption spectrum of G2 overlays that of G7 and is not shown.

The oscillator strength *f* of a cyanine dye is straightforward to calculate and is known to approach unity having been estimated to be 1.02 for the non-carboxylated analogue of G2.[20] A similar calculation for **N3** in the visible is more difficult because of overlapping absorption bands with differing origin.[14] However, an upper limit to *f* of 0.143 for the 490 transition has been estimated if it is assumed that the entire visible absorption is one band.[17] It is evident that these cyanine dyes have *f* values which exceed that of the **N3** dye by a factor of 3 to 4. From the perspective that each binding site in the TiO_2 layer now has an optical cross section several times greater than **N3**, the greater absorption strength of these dyes allows for a correspondingly thinner nanocrystalline solar cell, as is demonstrated in this work.

Spectra are given in Figure 3 for B1, G7, and R4 in 4 μm TiO_2 layers. The absorption spectra of dyes attached to TiO_2 differs from that found for the dyes in solution. There is the expected red shift of the monomer absorption maximum of the dye on the surface relative to its solution maximum, but there is also a pronounced absorption by the blue shifted H-aggregate peak. The relative magnitude of these peaks reveals the extent of aggregation of the dye on the surface and is a function of time of immersion of the nanocrystalline substrate in the dye solution.

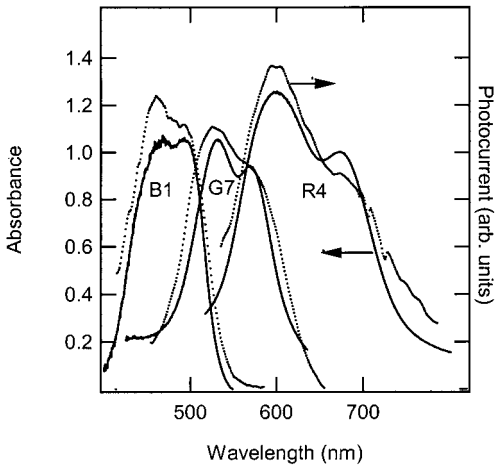

Figure 3. Absorption spectra are given for 4 μm TiO_2 nanocrystalline layers on F-doped SnO_2 that have been immersed in ethanolic solutions of the B1, G7, and R4 dyes for several hours. Dye concentrations were 5×10^{-5} M and higher. Also provided are photocurrent action spectra of these same electrode layers when assembled in a solar cell and illuminated under short circuit configuration. The action spectra have been normalized to the unit incident photon and are seen to follow the absorption spectrum of the dyes, confirming that the aggregate and monomer forms of the dyes sensitize with equal efficiency. The quantum efficiency for current production was found to 70% (±7%) for B1 and G7 and 8.0% for R4 (±1%)

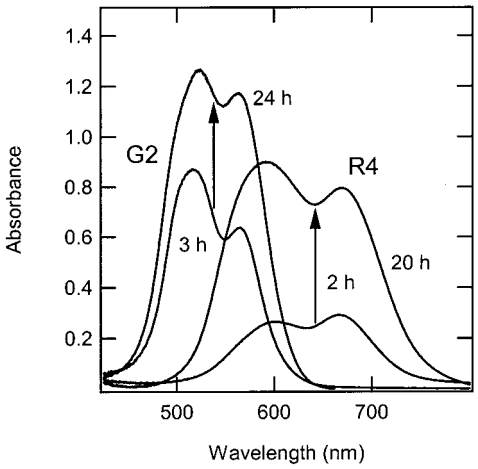

Figure 4. The time dependence of the attachment of dyes to nanocrystalline TiO_2 can differ from dye to dye. The time evolution of the absorption spectra of G2 and R4 show that the blue-shifted aggregate form of R4 comes into prominence with time, whereas the reverse is true for G2. These spectra were recorded for the same TiO_2 samples as a function of their immersion time in concentrated ethanolic solutions of the dyes.

Two distinct behaviors of the dyes manifest themselves when surface coverage is less than unity. In one, the initial dye adsorption is preferentially as a monomer with subsequent attachment leading to growth in H-aggregation. This behavior is typical of R4 and is shown in Figure 4. The second trend is the reverse. The dye attaches initially in an aggregated state and then gradually reverses its preference as the monomer grows in the spectrum. This is depicted in Figure 4 for the case of G2. B1, G6, and R4 fall into the former category; G7 and R5 fall into the latter.

An additional observation is the contrast in H-aggregation of R4 as opposed to the remaining dyes. R4 exhibits a broad H-aggregate, one typical of that found for cyanine dyes on ZnO, TiO_2 single crystals, and silver halide grains.[22−24] The other dyes, however, show sharply defined blue-shifted peaks indicative of formation of only the dimer, or with limited further aggregation. This limited aggregation could occur if the binding sites for neighboring dyes were greater than van der Waals distances and the molecules aggregated by leaning toward one another, which would limit dye−dye interactions to pairs of dyes.

TABLE 1: Dye Redox Potentials (mV vs Ag/AgCl)

	$E^o_{D+/D}$	$E^o_{D+/D*}$
B1	+1052	−1597
G2	+930	−1415
G6	+722	−1472
G7	+997	−1482
R4	+668	−1241

TABLE 2: Thickness Dependence of Solar Cell Performance Parameters

	R5		N3	
thickness (μm)	i_{sc} (mA/cm^2)	V_{oc} (mV)	i_{sc} (mA/cm^2)	V_{oc} (mV)
0.9	1.8	380	2.1	385
2.3	3.6	450	3.9	440
3.9	4.3	475	6.3	475
5.1	5.4	460	7.8	460
8.1	5.7	400	9.1	400
10.5			9.4	400

The energetics of the excited state of cyanine dyes are known to be favorable for electron transfer to the TiO_2 substrate. The excited-state oxidation potential $E^o_{D+/D*} = E^o_{D+/D} + h\nu$ for all these dyes was derived from the measured oxidation potentials of the dyes and the absorption spectra of the monomer form of the dyes when attached to the TiO_2 surface. The results are listed in Table 1 for selected dyes and show that the presence of the carboxyl groups shifts $E^o_{D+/D}$ by only about 30 mV from the potentials of their non-carboxylated analogues.[25] As has been shown by Lenhard,[25] $E^o_{D+/D}$ for a cyanine dye can change upon adsorption to a solid, but this change appears to be in the 50−100 mV range. In each case, $E^o_{D+/D*}$ is more negative than the conduction band energy of the nanocrystalline TiO_2, which has been estimated by Gratzel at −400 mV (Ag/AgCl).[26]

The absorption spectra of the dyes on the nanocrystalline TiO_2 were measured for each dyed TiO_2 layer that was to be used in a solar cell. The examples of Figure 3 are typical for the solar cells tested. For the initial pass at solar cells, 10^{-4} M, or saturated solutions of the dyes in dry ethanol were used. The coated TiO_2 layers were inserted into these solutions and allowed to soak for 8−12 h. The dyed coatings were highly colored.

The sensitizing ability of the dye in a solar cell is a compound function of the light harvesting ability of the dye and the efficiency of electron transfer from the excited dye to the nanocrystalline solid. A crude measure of this sensitizing ability can be found in the short circuit photocurrent of the solar cell.

A thickness of 4 μm was selected for the solar cells of this work, because it was at this thickness that diminishing returns in short circuit photocurrents was observed as a function of cell thickness. This result is expected because of the high f values for the dyes. These thickness studies were done with cells that varied in thickness from 1 to 8 μm, and that used a variety of these cyanine dyes. **N3**-dyed TiO_2 served as a control. We compare a typical result, that of R5 with the **N3** dye in Table 2 where it is seen that short circuit photocurrents saturate at a lower thickness for R5 than for **N3**.

In Table 3 are listed typical short circuit photocurrents for **N3** and the cyanine dyes of Figures 4−6 in a 4 μm cell. Fill factors ranged from 70 to 90%. It is evident from Table 3 that

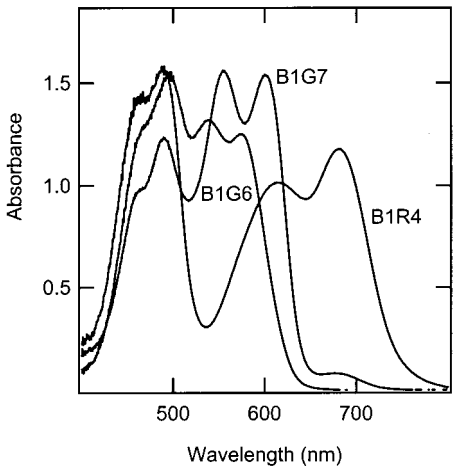

Figure 5. The absorption spectra are given for mixed dye attachment to TiO_2. The dyes are attached in sequence to the TiO_2 through successive immersion in solutions of the red absorbing dye followed by B1. The resulting absorption spectra are a function of the dye solution concentration and time of immersion in each solution.

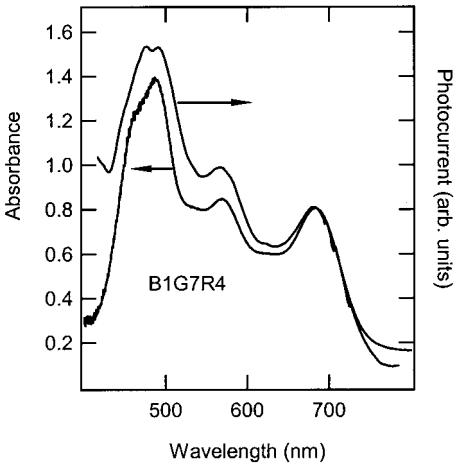

Figure 6. Absorption and photocurrent action spectra are given for a mixture of three dyes attached to nanocrystalline TiO_2 through immersion in ethanolic solutions of R4, G7, and B1, ranging from 5×10^{-4} M to 1×10^{-4} M in concentration. The photocurrent action spectrum recorded for a solar cell in a short circuit configuration, normalized for unit incident photon, follows the absorption spectrum of the attached dye. This correlation proves that all forms of all dyes, monomer or aggregate, sensitize with equal quantum efficiency for current production, which was measured to be 10%.

TABLE 3: Typical Short Circuit Photocurrents (i_{sc}) and Open Circuit Voltage (V_{Oc}) for 4 μm Layers 250 W Tungsten−Halogen Lamp W/420 nm Cutoff Filter

	i_{sc} (mA/cm^2)	V_{oc} (mV)
B1	2.8−3.4	525
G2	3.2−3.4	465
G6	4.8−6.2	425
G7	5.9−6.4	450
R4	1.8−2.1	380
R5	4.9−5.7	425
N3	5.4−6.3	440

at the 4 μm thickness of the nanocrystalline layer, several of these dyes, G6, G7, and R5, yield photocurrents comparable with the **N3** dye.

The absorption spectra of the aggregated dye on the TiO_2 layers were found to match the action spectrum for the photocurrent, normalized to unit incident photon, when the dyed layers were used in a solar cell configuration. This is seen in Figure 3 for the B1, G7, and R4 on 4 μm thick TiO_2 layers. For B1 and G7 the quantum efficiency for current production was measured to be 70% (± 7%); for R4, it was found to be 8.0% (± 1%). The aggregate sensitization appears to be as efficient as that of the monomeric forms of the dye.

TABLE 4: Mixed Dye Solar Cells at 4 μm Thickness

	i_{sc} (mA/cm^2)	V_{oc} (mV)	
B1G7	8.3	480	
B1G6	4.3	440	
B1R4	6.4	425	
B1R5	6.5	450	
G6R4	5.7	475	
B1	2.2	460	(control)
G7	5.9	440	(control)
R5	5.7	425	(control)
N3	6.3	490	(control)

TABLE 5: Influence of TiO_2 on Dye Mixture Spectra (nm)

dye mix	B1 H λ_{max}	B1 M λ_{max}	H λ_{max}	M λ_{max}
B1G6	458	484	558	599
dyes singly	458	486	547	586
B1R4	458	486	629	680
dyes singly	458	486	587	663

The cells averaged 3.5 cm^2 in size, and it is evident that great improvement could be made in these solar cells; the photovoltage is low and the slope of the current−voltage curve near the photovoltage intercept is low, indicating excessive resistance in the cell. Inspection of the dyed nanocrystalline solids reveals the presence of micron-sized agglomerations of the nanoparticles. The nonuniformity of the coating can also exceed 10% which prevents a uniform contact of the counter electrode with the nanocrystalline electrode over the entire surface. At lower currents, the fill factors of typical cells approached 90%; whereas they suffer at high current densities, falling to about 70%. An estimate of the photoconversion efficiency of the best **N3** cell was 4%, this done without the addition of any additives, such as the pyridine derivatives, to enhance V_{oc}.

Each of these cyanine dyes absorbs only a fraction of the solar spectrum so that a combination of several dyes is necessary to absorb light over the entire visible spectrum. Spectral studies were made of mixtures of these dyes on nanocrystalline TiO_2. The sintered TiO_2 layers were immersed in dye solutions in a sequential manner, beginning with the red-most absorbing dye. The TiO_2 layer was immersed in a solution until it acquired the desired absorption characteristics and then inserted into the next solution. It was observed that the spectral maximum of the most red absorbing dye of a combination of dyes was shifted to a longer wavelength than when present alone. The spectral maxima of combinations of dyes are given in Table 5 along with the maxima of the single dyes alone.

Solar cells were made using combinations of dyes on 4 μm layers, and their absorption spectra and current−voltage curves measured. Spectra of specific combinations of dyes are given in Figure 5. Only limited studies of mixed dyes were pursued because of the great dependence of the results on the order of immersion of the dyes and the length of time in each dye solution. After 8 h periods, some dyes, such as B1 will displace other dyes, or will disrupt aggregation of another.

Characteristics of these and other mixed dye solar cells are given in Table 4 for a 4 μm thickness and reveal photocurrents that can equal those of the **N3** dye at 10 μm thickness. Along with the mixtures, individual cells of the component dyes were also made as controls. The sum of currents from solar cells of the individual dyes was found to match the current from the

cell containing both dyes attached to the TiO_2 in sequence, although variations were found. In part, this can be attributable to the changed absorption spectrum of the dyes when present in mixtures on the TiO_2 surface. Such changes are evident in Table 5, which lists a comparison of the spectral maxima of the dye mixtures B1G6 and B1R4 with those for the individual dyes. It is seen that the both peaks of the red-most dye of a mixture are red-shifted from behavior of the dye alone, showing that the mixed dye system absorbs light in a different spectral region than the sum of the two individual dyes. Such behavior may be attributable to attachment of the dyes in dye mixtures at different locations on the TiO_2 than they would attach when used alone.

Use of three dyes and even more is possible, and is desirable, since the spectral absorption can then be extended arbitrarily into the near-IR region of the spectrum. The limiting factor then becomes, of course, the ability of the excited dye to inject electrons into the conduction band of the TiO_2; in general, the further into the near-IR that a cyanine dye absorbs, the more positive the oxidation potential of the excited state.[27] We show here in Figure 6 the correlation between the action spectrum of a three-dye mixture of B1G7R4 with its absorption spectrum on the TiO_2. The quantum efficiency of current production was measured at 10% for this particular cell. Once again we obtain the result that the aggregate forms of the dye are efficient light harvesting elements.

Discussion

These organic dyes attach themselves easily to the nanocrystalline TiO_2 surface and yield absorption spectra characteristic of both monomeric and aggregate forms. These forms are evident in the two-peaked spectra of Figures 3, 4, and 6 where the red peak corresponds to a monomer absorption and the blue-shifted peak to an H-aggregate. No J-aggregates were seen with these dyes, although extensive work was done to manipulate the adsorption conditions so as to favor such an event. In other laboratory work, dyes substituted symmetrically at the 5, 5′ positions with chloro, methoxy, and methyl functions, which are known to favor J-aggregation on silver halide surfaces, showed no tendency to form J-aggregates on nanocrystalline TiO_2. The strong interaction involved in the attachment of the dyes to the TiO_2 through the carboxyl groups appears to dominate the subtle dye-dye interactions involved in the formation of the red-shifted J-aggregate.

The high oscillator strength of these dyes leads to the behavior observed in Table 2 where the short circuit photocurrents of the dye R5 are seen to peak between 4 and 5 μm thickness, whereas the control **N3** cell required an 8 μm thickness. The absorption spectra of Figures 3 and 4 show that the extinction of the dyes at this 4−5 μm thickness exceeds 1.0 and that any further increase in thickness provides only a marginal increase in light harvesting.

The spectral width of these dyes is much narrower than that of the **N3**. Therefore an increase in light harvesting can only be brought about through the use of several of the cyanine dyes which together cover the entire visible spectrum. We have been successful in combining several of these dyes together in a spectral sensitization package to cover the visible region. This is seen in Figure 5 where various combinations of dyes have been attached to nanocrystalline TiO_2 yielding an absorption that spans the visible from 450 to 700 nm. These mixed dye TiO_2 layers can appear black, as in the B1G7 cell, green as with the B1R4 cell, or reddish in color, as seen with a B1G6 cell.

Their short circuit photocurrents vary somewhat, from 4 to above 8 mA/cm^2, as is seen in Table 4. This variation must reflect not only the spectral extent of the light harvesting, but also the effects of the various aggregated dyes upon the efficiency of the electron injection reaction. We draw attention in Figure 3 to a comparison of dimer-dominated spectrum of G7 with the broad H band of R4, which represents a heterogeneous absorption band of a collection of H-aggregates of different length. The wide assortment of aggregates seen for R4 may provide an efficient quenching mechanism for electronic excitation and be responsible for the lower i_{sc} for this dye as compared to G7. It is also possible, as Sauve et al.[28] have shown, that at this high dye coverage, the low i_{sc} may be controlled by a fast velocity for the back reaction between injected electron and the hole state of the dye. This velocity may be greater with this heterogeneous assortment of R4 aggregate forms than for the more limited number of aggregates for G7 or R5.

At 8.3 mA/cm^2 for a 4 μm thick cell using B1G7, however, the i_{sc} of these cells compares well with the short circuit photocurrent of **N3** at 4 μm, which is only about 6 mA/cm^2 in the solar cells of this work. With thicker cells the i_{sc} for **N3** only increases to 8−9 mA/cm^2. Combinations of organic dyes, such as these cyanines, merit study as sensitizers in these dye-sensitized solar cell systems.

It was also found that the spectral characteristics of these dyes also provide more information about the attachment process than the **N3** species with its broad spectral width. The relative degree of monomer and aggregate absorption of these dyes as a function of attachment conditions yields the concentration dependence of formation of each form. The spectra of Figure 4 show how the tendency toward aggregate or monomer can vary from one dye to the next. The degree of aggregation of the dye appears to depend on the structure of the chromophore as well as the nature of the particular carboxylic acid chelation function.

When several dyes are attached from a mixed solution of dyes, some dyes such as oxacarbocyanine dye B1 dominate the resultant spectrum at longer immersion times of the TiO_2 in the dye solution, revealing a displacement of analogous thiacarbocyanine dyes that dominate the spectrum at shorter times. This has been shown in recent work[17] where the relative degree of attachment of these dyes and their aggregation was followed easily because of the distinctive spectral characteristics; the effect of different carboxylic acid function linkages on the absorption spectrum and on conversion efficiencies was explored. Comparisons of dyes with propanoic, acetic, and methyl benzoic acid chelation were made. One concludes, for example, that the betaine function of the G7 chelation appears to bind the dye more tightly to the surface than the G2 propionic function. The G7 spectrum is broader in width and the G7 i_{sc} is greater than that of G2.

Aggregates of dyes can play a dual role in the spectral sensitization of solids. One role is as a light-harvesting antenna, where they serve only to absorb light and, through energy transfer, funnel this energy to the reddest absorbing species on the surface, from which electron transfer occurs. This appears to be the case for the spectral sensitization of silver bromide by J-aggregates of cyanine dyes.[29] Another role is for electron transfer to occur from each chromophore in the assembly of adsorbed dye. In the first case the relative efficiency of the aggregate and monomer would be equal if energy transfer from the aggregate to the monomer were 100% efficient. In the latter case, electron transfer would occur from the excited aggregate to the TiO_2 as well as from the monomer. In this case, if the quantum yield for sensitization were different for these two

forms of the dye, the action spectrum would not match the absorption spectrum of the attached dye. The results of this work do not show this. The normalized action spectra do match the absorption spectra as Figures 3 and 6 show. However, this does not give an unambiguous indication of the role of the aggregates in spectral sensitization. If electron transfer for both monomer and aggregate forms of the dye were sufficiently fast, the quantum yield for electron transfer could be equal.

The redox potential data for the excited state in Table 1 reveal that for all of the dyes under study, and their aggregates, the excited-state donor levels overlap the conduction band of the TiO_2. Therefore, the electron transfer from each of these dyes to TiO_2 should be activationless, as it is for **N3** and might be expected to occur with the same subpicosecond rate. For **N3**, electron transfer with this energetic overlap has been reported to occur within 50 fs of photon absorption, which is faster than intersystem crossing to the triplet state.[30]

Work with perylene sensitizers for nanocrystalline substrates has shown that the electron transfer to the solid occurs before thermal equilibration of the excited state.[31] Therefore, the ability of the excited sensitizer can no longer be described by E^o_{D+/D^*}, but rather by the total energetic overlap of the spectral distribution function of the excited state with the acceptor states of the TiO_2 conduction band.

In a similar manner, it is possible, with a femtosecond electron-transfer time, that all aggregated forms of the dye on the surface can transfer electrons to the TiO_2 before any internal relaxation, internal conversion, or energy transfer to the monomer can occur. However, it is impossible to characterize the photophysics of the many aggregate forms of the dye to the degree that **N3** has been characterized, and it is not known how fast these internal relaxation and energy transfer processes occur within these many aggregates. The only experimental approach for confirming fast electron transfer from an aggregate would be through picosecond absorption studies of the injected electron within the conduction band of the TiO_2, as Ellingson et al. have done.[32−33]

It is also possible that the blue-shifted aggregates of the dyes in Figures 3 and 5 and the blue absorbing dyes of Figure 6 will transfer their excited-state energy to the furthest red component of the absorption spectrum, from which the electron transfer occurs. This is what is observed for J-aggregates of cyanine dyes on AgBr microcrystals.[29] Such an antenna complex would also exhibit an action spectrum that matches the absorption spectrum of the attached dye. This ambiguity in the role of the aggregates will remain until the picosecond absorption studies have been done. From the perspective of solar energy conversion, the antenna arrangement with fast energy transfer would be less desirable because the photocurrent would funnel through only a few dye molecules on each surface. This would not be a durable arrangement because the system could become disabled through destruction of these few dye molecules.

Acknowledgment. This study was supported by the U.S. Department of Energy under Contract 98ER82552.

References and Notes

(1) Nazeerudin, M. K.; Kay, A.; Rodico, I.; Humphry-Baker, R.; Müller, E.; Liska, P.; Vlachopoulos, N.; Grätzel, M. *J. Am. Chem. Soc.* **1993**, *115*, 6382.
(2) Smestad, G.; Bignotti, C.; Argazzi, R. *Sol. Ener. Mater.* **1994**, *32*, 259.
(3) Nazeerudin, M. K.; Pechy, P.; Grätzel, M. *J. Chem. Soc., Chem. Commun.* **1997**, *18*, 1705.
(4) U.S. Patent 6,043,428 (2000); U.S. Patent 6,028,265 (2000).
(5) Kay, A.; Grätzel, M. *J. Phys. Chem.* **1993**, *97*, 6272.
(6) Boschloo, G.; Goossens, A. *J. Phys. Chem.* **1996**, *100*, 19489.
(7) Kalyanasundaram, K.; Vlachopoulos, N.; Krishnan, V.; Monnier, A.; Grätzel, M. *J. Phys. Chem.* **1987**, *91*, 2342.
(8) Tachibana, Y.; Haque, A. A.; Mercer, I. P.; Durrant, J. R.; Klug, D. R. *J. Phys. Chem. B* **2000**, *104*, 1198.
(9) Nazeeruddin, M. K.; Humphry-Baker, R.; Grätzel, M.; Murrer, B. A. *Chem. Commun.* **1998**, 719.
(10) Shen. Y.; Wang, L.; Lu, Z., Wei, Y.; Zhou, Q.; Mao, H.; Xu, H. *Thin Solid Films* **1995**, *257*.
(11) Cherian S.; Wamser, C. C. *J. Phys. Chem. B* **2000**, *104*, 3624.
(12) Kamat, P. V.; Hotchandani, S.; Lind, M.; Thomas, K. G.; Das, S.; George, M. V. *J. Chem. Soc., Faraday Trans.* **1993**, *89*, 2397.
(13) Sayama, K.; Sugino, M.; Sugihara, H.; Abe, Y.; Arakawa, H. *Chem. Lett.* **1998**, 753.
(14) Wang, A.-S.; Li, F.-Y.; Huang, C.-H.; Wang, L.; Wei, M.; Jin, L.-P.; Li, N.-Q. *J. Phys. Chem. B* **2000**, *104*, 9676.
(15) Nuesch, F.; Moser, J. E.; Shklover, V.; Grätzel, M. *J. Am. Chem. Soc.* **1996**, *118*, 5420.
(16) Liu, D.; Kamat, P. V. *J. Electrochem. Soc.* **1995**, *142*, 835.
(17) Ehret A.; Stuhl, L.; Spitler, M. T. *Electrochim. Acta* **2000**, *45*, 4553.
(18) Lenhard, J. *J. Imag. Sci.* **1986**, *30*, 28.
(19) U.S. Patent 5,463,057 (1995).
(20) West, W.; Geddes, A. L. *J. Phys. Chem.* **1964**, *68*, 837.
(21) Juris, A.; Balzani V.; Bargelletti, F.; Campagna, S.; Belser, P.; Zelewsky, A. *Coord. Chem. Rev.* **1988**, *84*, 85.
(22) Kavassalis, C.; Spitler, M. T. *J. Phys. Chem.* **1983**, *87*, 3166.
(23) Sonntag, L. P.; Spitler, M. T. *J. Phys. Chem.* **1985**, *89*, 1453.
(24) Ehret, A.; Kietzmann, R.; Spitler, M. T.; Willig, F. *J. Am. Chem. Soc.* **1993**, *115*, 1930.
(25) Lenhard, J. R.; Hein, B. R. *J. Phys. Chem.* **1996**, *110*, 17287.
(26) Rothenberger, G.; Fitzmaurice, D.; Grätzel, M. *J. Phys. Chem.* **1992**, *96*, 5983.
(27) Lenhard, J. R.; Hein, B. R.; Muenter, A. A. *J. Phys. Chem.* **1993**, *97*, 8269.
(28) Sauve, G.; Cass, M.; Coia, G.; Doig, S. J.; Lauermann, I.; Pomkyal, K. E.; Lewis, N. *J. Phys. Chem. B* **2000**, *104*, 6821.
(29) Trosken, B.; Willig, F.; Schwarzburg, K.; Ehret, A.; Spitler, M. T. *J. Phys. Chem.* **1995**, *99*, 5562.
(30) Hannapel, T.; Burfeindt, B.; Storok, W.; Willig, F. *J. Phys. Chem. B* **1997**, *101*, 6799.
(31) Burfeindt, B.; Zimmermann, C.; Ramakrishna, S.; Hannapel, T.; Meissner, B.; Storck, W.; Willig, F. *Zeit. Physik. Chem.* **1999**, *212*, 67.
(32) Ellingson, R. J.; Asbury, J. B.; Ferrere, S.; Ghosh, H. N.; Sprague, J. R.; Lian, T.; Nozik, A. J. *J. Phys. Chem. B* **1998**, *102*, 6455.
(33) Ellingson, R. J.; Asbury, J. B.; Ferrere, S.; Ghosh, H. N.; Sprague, J. R.; Lian, T.; Nozik, A. J. *J. Phys. Chem. B* **1999**, *103*, 3110.